Unfolding the AmBe Neutron Spectra using GRAVEL and MLEM

Tyler D. Doležal[1]

***Abstract*— In this work I implement two unfolding algorithms, GRAVEL and MLEM, in Python3. As validation, the algorithms were used to unfold the neutron spectra of AmBe and results were compared against a neutron time of flight AmBe energy spectrum. Results show that both algorithms succeed in unfolding the spectra of AmBe off of an experimentally captured pulse height data set. The time of flight experiment, unfolding data collection, and algorithm details are discussed within.**

I. Introduction

During this project three major efforts made, (1) performing a time of flight (ToF) experiment, (2) collecting a substantial amount of data from an Americium-Beryllium (AmBe) source, and (3) implement a neutron spectrum unfolding algorithm in Python 3. Each of these subprojects will be discussed in the following sections. First, it is best to motivate the purpose of sub-project (1) and (3).

A. Time of Flight

The primary focus of the research was to develop a neutron unfolding algorithm and use it on AmBe. In order to validate the unfolded results, the AmBe spectra will be reported an alternate way: by use of a ToF experiment. ToF experiments allow for timing of a neutron's flight over a distance set by the user. One detector is placed close to the source, this acts as the stopwatch start button and another detector is placed a considerable distance away, this acts as the stopwatch stop button. The further the stop detector is placed, the better the energy resolution, as demonstrated by the error propagation relationship,

$$\left(\frac{\Delta E_n}{E_n}\right) = \sqrt{\left(\frac{2\Delta d}{d}\right)^2 + \left(\frac{2\Delta t}{t}\right)^2}$$

where Δd is the uncertainty in the neutron's traveled distance, which depends mainly on the detector size, and Δt is the timing resolution of the experimental system. In most cases, the user has most control over d, the distance between source and stop detector, and so it is the parameter easiest to optimize. Because AmBe is a (n,γ) source, there are four events that can occur,

$$1.\ \gamma,\gamma \qquad 2.\ \gamma,n \qquad 3.\ n,\gamma \qquad 4.\ n,n$$

where the order of the particle type indicates start-capture, stop-capture. The γ,γ events offer insight into the electronic signal processing delay and the γ,n events are where the spectrum data comes from. AmBe neutrons are generated through the interaction of a ^{241}Am-generated α particle interacting with the ^{9}Be nucleus, shown in the expression below,

$$\alpha + {}^{9}_{4}\mathrm{Be} \rightarrow {}^{13}_{6}\mathrm{C}^{*} \rightarrow {}^{12}_{6}\mathrm{C} + \mathrm{n} + \gamma(4.44\ \mathrm{MeV})$$

. The γ,n event is the 4.44 MeV photon starting the stopwatch and the neutron stopping the stopwatch, after traveling the distance, d, to the stop-detector. The maximum possible energy a neutron can have is $Q+\langle T_\alpha\rangle$ = 11.188 MeV, which, for a neutron, is a speed of about 0.11c. Therefore, it is valid to use the non-relativistic formulation of kinetic energy for the neutron energy,

$$E_n = \frac{1}{2}m_n\left(\frac{d}{t}\right)^2 \tag{1}$$

where d is the distance from source to stop-detector and t is the time from the start-detector collecting the 4.44 MeV γ and the stop-detector detecting the neutron. There is always the possibility of chance coincident events, as well, which typically occur in time regimes far too quickly or much too slow to be true γ,n events; this makes them easy to discriminate.

B. Neutron Spectrum Unfolding

Spectrum unfolding is an alternative to conducting a ToF experiment. In some cases, it could be that a ToF experiment isn't possible. One such scenario is in a nuclear reactor. Nuclear reactor design and safety is an area of industry interested in neutron unfolding due to the spectrum being a key input when dealing with criticality, dose protection, and fuel consumption. There are many different unfolding algorithms already developed, FERDOR [1], MAXED [2], GRAVEL [3], MLEM [4], and a machine-learning based algorithm [5]. This project implements GRAVEL and MLEM using Python 3. How these two algorithms work will be discussed in more detail in the following sections. For now, the concept of the unfolding algorithm is to solve **Ax** = **b** where the dimensions are: [**A**] = (n x m), [**x**] = (n x 1), and [**b**] = (m x 1). Typically, n >> m, so this is an over-determined problem; meaning, there are many possible solutions to this problem. **A** is commonly referred to as the response matrix and is specific to each detector, **x** is the source's neutron energy spectrum, and **b** is the pulse height spectrum collected by the detector. The goal of the unfolding algorithm is to sort through all the potential **x** spectra and find the best one.

II. Experimental Effort

A. Time of Flight

AmBe data was recorded using two 2" Eljen EJ-309 liquid organic scintillators [6], both of which were attached to a

[1]Department of Engineering Physics, Air Force Institute of Technology

2" Hamamatsu photo-multiplier tube (PMT). The detectors were connected to a CAEN DT5730 digitizer [7] and a DT5533 high voltage power supply [8]. The voltage was set to 1100 V using GECO [9] and was not changed throughout the collection process. Data acquisition and PSD parameters were set using CAEN Multi-Parameter Spectroscopy Software (CoMPASS) [10]. The start-detector was placed 0.027 m from the source and the stop-detector was placed 1.35 m from the source. Table I gives all of the settings that were set using CoMPASS.

TABLE I

THE SETTINGS USED FOR DATA ACQUISITIONS

	CoMPASS Setting	Value
Input	Record Length (ns)	400
	Pre-trigger (ns)	96
Discriminator	Mode	Leading Edge
	Threshold (LSB)	1000
	Trigger Hold Off (ns)	400
QDC	Long Gate (ns)	350
	Short Gate (ns)	60
	Pre Gate (ns)	20
CI	Coincident Mode	Paired AND
	Coincident Window (ns)	400

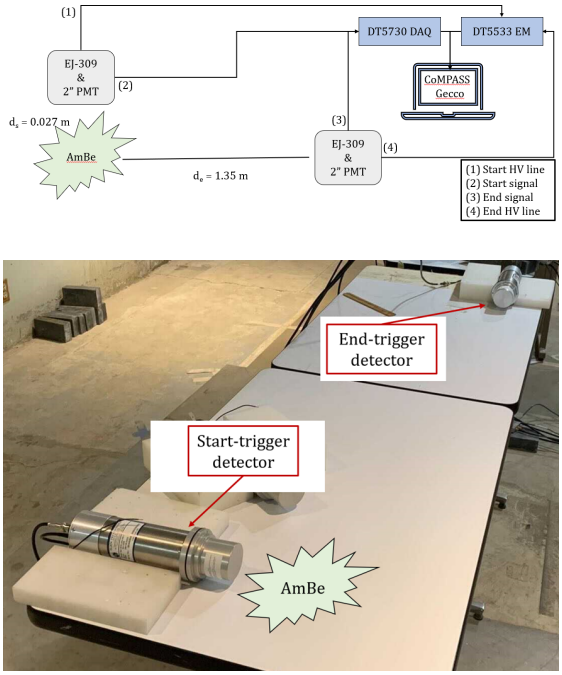

Fig. 1. (Top) A diagram of the data acquisition system set up for the AmBe data collection; not to scale. (Bottom) A photograph of how the detectors were placed for the AmBe data collection.

A diagram of the detection system and a photo of the detectors' placement is shown in Figure 1 (Top), (Bottom) respectively. The data was recorded over a 24-hour period and resulted in 66,902 coincident events.

The first step of the analysis process was to calculate the pulse-shape discrimination paramter (PSD) [11] for the start and stop detector data sets using the following expression,

$$\text{PSD} = 1 - \frac{Q_{\text{short}}}{Q_{\text{long}}}$$

and plot the 2D histograms. These are shown in Figure 2 where the start and stop detector correspond to (Top), (Bottom).

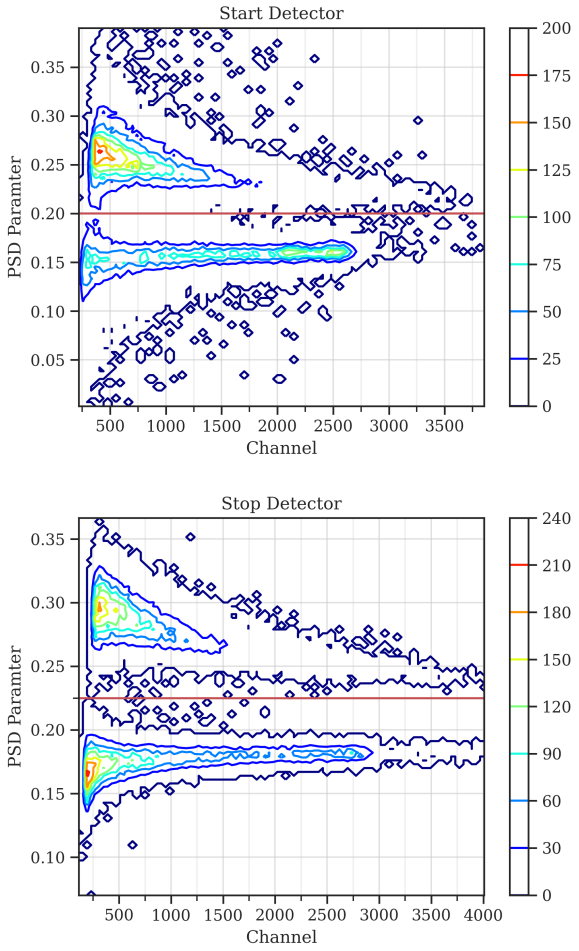

Fig. 2. (Top) The 2D histogram for the start detector data set. The chosen PSD value for making a cut is marked with a red horizontal line, PSD = 0.2, in this case. (Bottom) The 2D histogram for the stop detector data set with the PSD = 0.225 cut marked by a red horizontal line.

From these histograms, it was determined that a PSD discrimination value of 0.2 for the start detector and 0.225 for the stop detector were suitable for distinguishing between γ and neutron events. PSD discrimination was used to separate into four events, listed below.

1. γ, γ $\quad \text{PSD}_0 \leq 0.2,\ \text{PSD}_f \leq 0.225$
2. γ, n $\quad \text{PSD}_0 \leq 0.2,\ \text{PSD}_f > 0.225$
3. n, γ $\quad \text{PSD}_0 > 0.2,\ \text{PSD}_f \leq 0.225$
4. n, n $\quad \text{PSD}_0 > 0.2,\ \text{PSD}_f > 0.225$

Once separated, the time difference between start-stop events was calculated and a Δt distribution was generated. From the

mean value of the γ, γ distribution, the signal process delay time was 25 ns. The Δt values were adjusted by adding 25 ns to them. An additional 4.5 ns were added to the Δt values to account for the γ time of travel from the source to the stop-detector 1.35 m away. Figure 3 shows the adjusted time histogram.

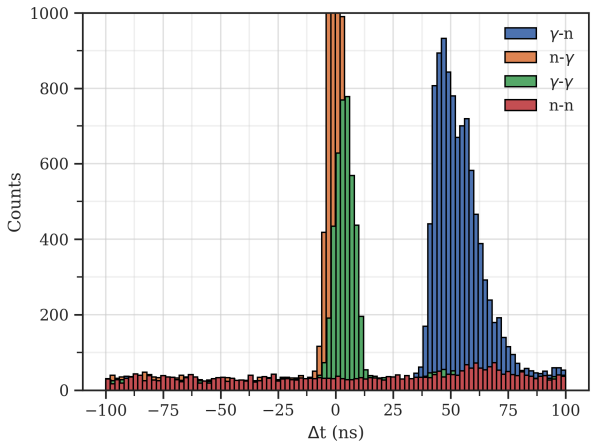

Fig. 3. The time-of-flight histogram for the four different events.

The neutron energy spectrum was calculated using Eq 1 and the Δt values reported in the γ,n time distribution.

B. AmBe Data Collection for Unfolding

AmBe unfolding data was collected using two EJ-309 detectors, as shown in Figure 4 (Top). The detector-to-source distances were not important for this collection. The electronics for this run are the exact same as those listed in the previous section. Data was recorded on a ^{137}Cs and ^{22}Na button source to provide a light calibration for both detectors. The points of calibration were, in order of energy, the ^{22}Na 339 keV, ^{137}Cs 477 keV, and ^{22}Na 1061 keV Compton Edges, which are highlighted in Figure 4 (Middle). The calibration was performed by finding the 1/2-max value of each Compton feature. This is a common method used for gamma-calibration of scintillators, but how close the 1/2-max value is to the true Compton edge does vary with detector size and resolution [12]. Light yield units are reported in keVee and MeVee which is a unit that rests on the assumption that the scintillator electron response is linear. The weakness of this assumption has been experimentally demonstrated [13]. Figure 4 (Bottom) shows the calibration equation for Detector 1 and 2, as labeled in Figure 4 (Top).

The AmBe data was processed through a means of PSD discrimination as discussed in the previous section. Only neutron events were used from this collection. The neutron pulse height spectra from Detector 1 and 2 were converted to units of MeVee using the best-fit equations reported in Figure 4. The neutron pulse spectra are shown in 5.

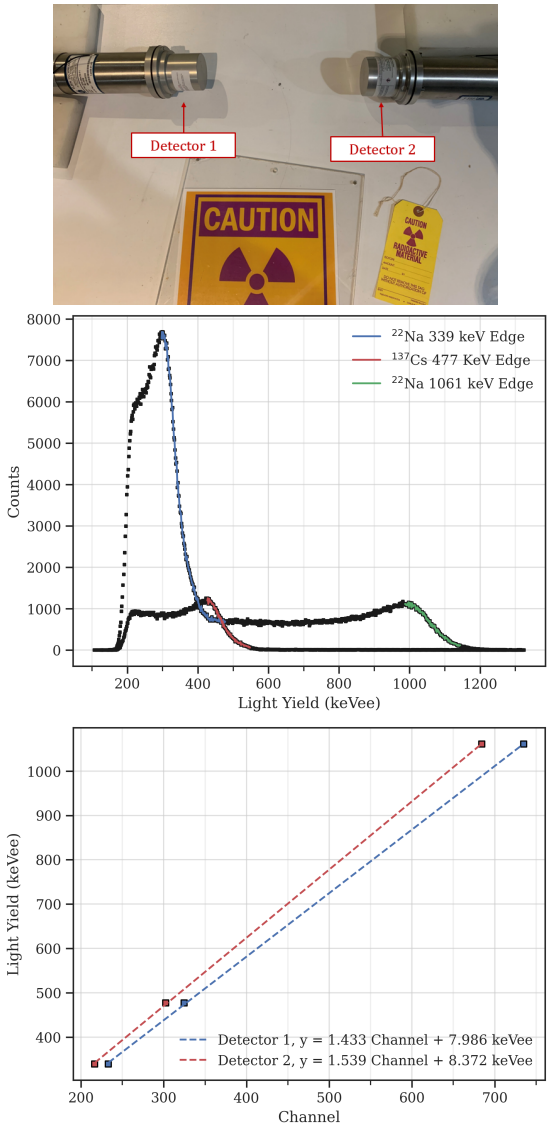

Fig. 4. (Top) AmBe data collection detector placement for unfolding data. The AmBe and gamma source(s) were placed on the gray dot marked on the table. (Middle) The pulse height spectrum from Detector 1 for the two gamma sources with the calibration sources labeled. (Bottom) The linear fit equations obtained from fitting to the Cs-137 and Na-22 Compton features as labeled above.

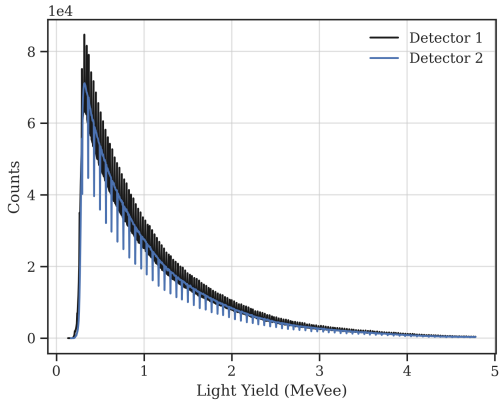

Fig. 5. The neutron pulse height spectra of the two detectors.

III. Neutron Spectrum Unfolding

A. GRAVEL

The GRAVEL algorithm requires four inputs, (1) a detector-specific response matrix, **R**, (2) an initial guess at what the neutron spectrum may be, **x**, (3) the pulse height spectrum used for unfolding, **N**, and (4) the tolerance required to terminate the algorithm. Table II has been provided to summarize the four inputs. Input (4) is usually between 0.1 and 0.9; the setting depends on the other three inputs and should be optimized. In my case, when using the ToF spectrum as the initial guess, I found 0.8 resulted in the best performance of the two algorithms when using Detector 1's pulse height spectrum, which is shown as the black line in Figure 5.

TABLE II
THE INPUTS THAT THE USER PROVIDES FOR THE GRAVEL ALGORITHM

Input	Indice	Shape	Units
Response Matrix	R_{ij}	(1024,201)	MeVee/MeV
Initial Guess	x_j	(201,1)	MeV
Pulse Height Spectrum	n_i	(1024,1)	MeVee
Tolerance	float value	–	–

In my case, **R** was generated by Captain Bryan Egner, a fellow AFIT student, for the EJ-309 organic scintillator. The neutron energies were binned into 201 bins and the light yield per energy was binned into 1024 bins. GRAVEL is an iterative solver and the solution vector is updated at each iteration according to the following equations,

$$x_j^{(k+1)} = x_j^{(k)} \exp\left(\frac{\sum_{i=1}^{n} W_{ij}^k \ln\left(\frac{N_i}{\sum_{l=1}^{m} R_{il} x_l^k}\right)}{\sum_{i=1}^{n} W_{ij}^k}\right)$$

where k is the kth iteration and the weight matrix, **W**, is given by,

$$W_{ij}^k = N_i \frac{R_{ij} x_j^k}{\sum_{l=1}^{m} R_{il} x_l^k}$$

and the residual is calculated using,

$$\frac{\chi^2}{n} = \frac{1}{n} \sum_{i=1}^{n} \frac{\left(\sum_{j=1}^{m} R_{ij} x_j - N_i\right)^2}{N_i}$$

The value, χ^2/n approaches one as the solution converges.

B. MLEM

The maximum-likelihood expectation maximization (MLEM) algorithm takes the same four inputs as GRAVEL. Like GRAVEL, it is an iterative solver, but does update the solution according to a different set of equations,

$$x_j^{(k+1)} = \frac{x_j^k}{\sum_{i=1}^{n} R_{ij}} \sum_{i=1}^{n} R_{ij} \frac{n_i}{\sum_{l=1}^{m} R_{il} x_l^{(k)}}$$

and uses a different convergence criteria, referred to as the MLEM-STOP [14],

$$J^{(k)} = \frac{\sum_{i=1}^{n} \left(n_i - q_i^{(k)}\right)^2}{\sum_{i=1}^{n} q_i^{(k)}}, \quad q_i^{(k)} = \sum_{j=1}^{m} R_{ij} x_j^{(k)}.$$

It has been reported that it is best practice to terminate the algorithm just before J reaches one [15].

C. Tolerance

Upon further investigation, I found that GRAVEL performed best when using MLEM's J convergence parameter. Rather than using a user-defined iteration limit, a stopping condition was used for both algorithms. The iterative solvers terminate when the absolute difference of the difference of J drops below a user-defined tolerance; typically somewhere between 0.1 and 0.9. That is,

$$\delta J^{(k+1)} = J^{(k)} - J^{(k+1)} \quad , \quad \Delta J^{(k+1)} = |\delta J^{(k)} - \delta J^{(k+1)}|$$

the algorithms terminate when $\Delta J <$ user-defined tolerance.

D. Preliminary Validation

Before executing GRAVEL or MLEM on real data a validation test was executed using the ToF spectrum, shown in Figure 7, as the true spectrum, $\mathbf{x}_{\text{ToF}}$. A pulse height spectrum, **N**, was generated using the equation $\mathbf{N} = \mathbf{R}\mathbf{x}_{\text{ToF}}$, and a constant spectra of ones was the initial guess. Figure 6 shows the GRAVEL, solid black line, and MLEM, dashed-dot orange line, unfolded spectra against $\mathbf{x}_{\text{ToF}}$, the shadowed black line.

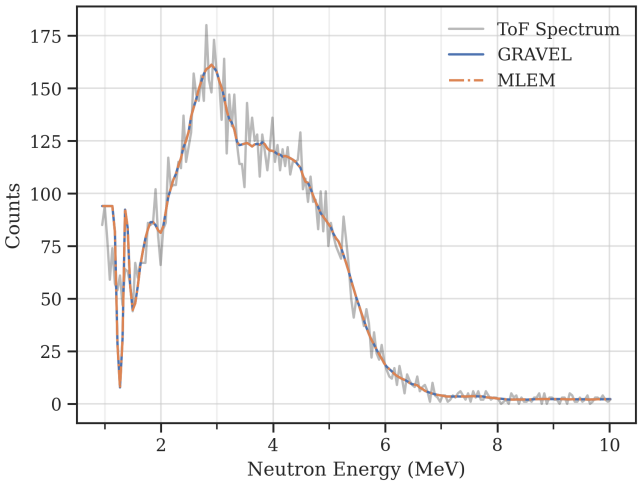

Fig. 6. GRAVEL, solid black line, and MLEM, dashed-dot orange line, unfolded spectra overlaid the ToF energy spectra when starting with an initial guess of a vector of all ones.

IV. Results & Analysis

A. Time of Flight

The result from the ToF experiment is the neutron energy spectrum, shown in Figure 7, which serves as $\mathbf{x}_{\text{ToF}}$ in the unfolding problem.

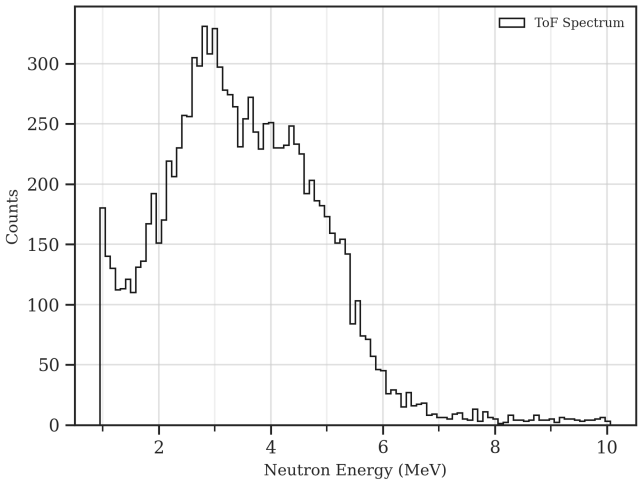

Fig. 7. The neutron energy spectrum obtained from the time of flight experiment.

B. Neutron Unfolding

The unfolding results are shown in Figure 8. Both algorithms perform poorly in the low energy regions of 0.1 to 2 MeV. GRAVEL fits the ToF spectrum very well between 2.5 and 6 MeV, while MLEM does not reach an adequate fit until close to 3 MeV. Seeing that both algorithms predict a higher 4 MeV neutron energy peak it is worth investigating if this does exist by collecting more ToF data. Another possibility is the response matrix could have a strong response in this energy range. To investigate this, a new response matrix should be constructed; preferably with fewer energy bins to avoid the statistical fluctuations that are present in the ToF spectrum from this work.

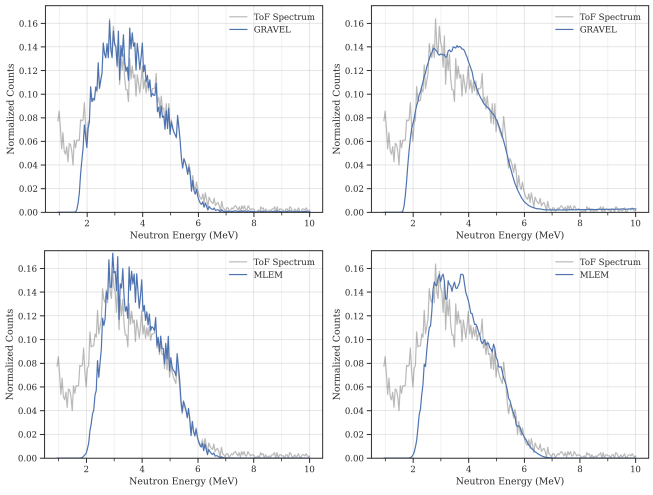

Fig. 8. (Top Left) Unfolding results from the GRAVEL algorithm when using the ToF energy spectrum as an initial guess. (Top Right) Unfolding results from the GRAVEL algorithm when using a constant spectrum of unity as an initial guess. (Bottom Right) Unfolding results from the MLEM algorithm when using the ToF energy spectrum as an initial guess. (Bottom Left) Unfolding results from the MLEM algorithm when using a constant spectrum of unity as an initial guess. All plots are plotted against the ToF spectrum, shown as a shadowed black line behind the unfolded results.

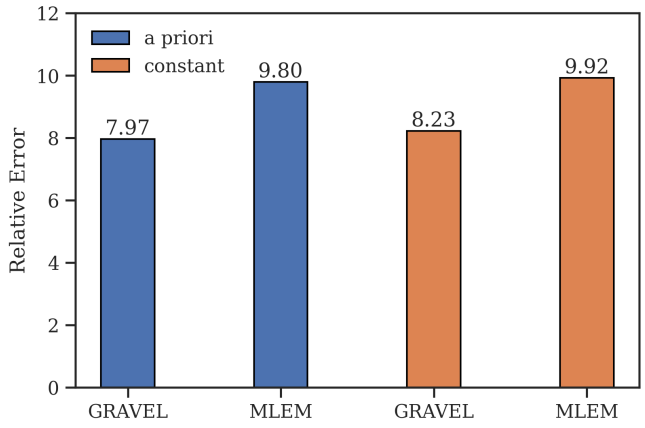

Fig. 9. The relative error of each algorithm for an a priori (blue) and constant (orange) initial guess.

To quantify the performance of each algorithm, the relative error was examined. The relative error vector is given by,

$$\epsilon_i^{\text{algo}} = \frac{|x_i^{\text{ToF}} - x_i^{\text{algo}}|}{x_i^{\text{ToF}}}$$

where the superscript algo refers to either GRAVEL or MLEM. Altogether, 4 relative error vectors were generated; one per algorithm per initial condition. In this case, the Frobenius norm of the relative error vector was defined as the relative error–the closer the norm is to 0, the better the unfolding algorithm performed. Figure 9 shows the relative error for each algorithm. The blue bars are when the ToF spectrum was the initial guess, and the orange bars are for the constant initial guess. It shows that GRAVEL performed the best for both initial guess cases.

The stopping condition was tested to determine what setting resulted in the best unfolded spectra. It was found that the stopping condition is sensitive to the initial guess; more so for MLEM than GRAVEL. In the case of the ToF initial guess, the unfolded spectra improved as the stopping condition approached 1; where any solution beyond 0.8 had negligible improvement. For the constant initial guess, the unfolded spectra improved as the stopping condition approached 0.1; where any solution less than 0.2 had a worse fit. This suggests that, when a good initial guess is provided, it is best to use a stopping condition closer to 1. Figure 10 has the stopping parameter, ΔJ, plotted against iterations for the a priori (Left) and constant (Right) initial guesses. Seeing that I have only attempted an unfolding on AmBe data, I hesitate to claim that either the switching of χ^2/n to J or the stopping parameter $\Delta J^{(k)}$ are universal improvements to the GRAVEL algorithm. To study this new stopping criteria more thoroughly I suggest executing the algorithms on other neutron sources with different neutron detectors. Two candidates available at AFIT are the ^{252}Cf source and AFRL's laser-generated neutron source.

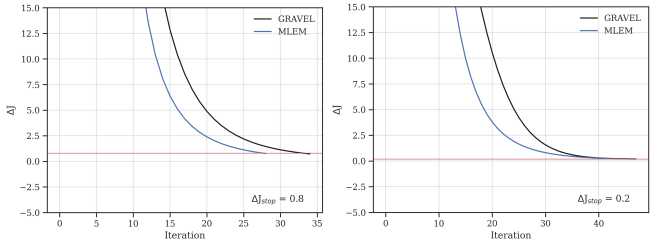

Fig. 10. (Left) The tolerance parameter for GRAVEL, black line, and MLEM, blue line, shown against iteration number when using the ToF spectrum as an initial guess. (Right) The tolerance parameter for GRAVEL, black line, and MLEM, blue line, shown against iteration number when using a constant spectrum of unity as an initial guess.

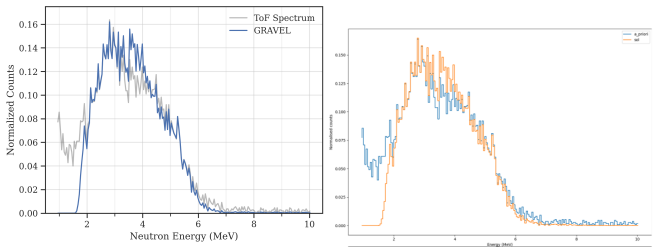

Fig. 11. (Left) The unfolded spectrum using the Python3 GRAVEL algorithm. (Right) The unfolded spectra of UF_G.

To measure the Python3 GRAVEL's performance as a GRAVEL unfolding algorithm, it was tested against a peer-reviewed GRAVEL algorithm, referred to as UF_G [16]. The comparison is shown in Figure 11, where (Left) is the Python3 and (Right) is UF_G. Both algorithms predict a very similar structure, with the biggest difference being seen around the neutron energy of 5 MeV. A key difference between the two algorithms is that the Python3 algorithm terminates based on the stopping condition while UF_G terminates based on a user-defined max iteration number. In this case, UF_G was terminated after 20 iterations and Python3-GRAVEL terminated after 33 iterations. The only data offered by the group responsible for UF_G was the image file of the unfolded result. Without the data file a relative error analysis was not able to be executed.

V. Conclusion

Using the time of flight spectra as reference, the Python3 GRAVEL and MLEM algorithms unfold the neutron spectra of AmBe with relative errors of (7.97, 9.80), respectively, when using an a priori initial guess, and (8.23, 9.92) when using a constant spectra as the initial guess. Both algorithms exhibit poor performance in the low energy range of 0.1 to 2 Mev. It is believed this could be due to EJ-309's insensitivity to low energy neutrons, but more analysis is required. From a relative error investigation, it is reported that GRAVEL unfolds a more accurate spectra over MLEM for both initial guess cases. When comparing Python3-GRAVEL against a peer-reviewed GRAVEL, the unfolded results were nearly identical, showing, (1) Python3-GRAVEL unfolds in true GRAVEL fashion and (2) the stopping condition terminates appropriately. Future work would see these two algorithms applied to new neutron sources using different neutron detectors. Two candidate sources are ^{252}Cf and a laser-generated neutron source held at Wright-Patterson AFB.

References

[1] W. R. Burrus and V. V. Verbinski, "Fast-neutron spectroscopy with thick organic scintillators," vol. 67, no. 2, pp. 181–196. [Online]. Available: https://www.sciencedirect.com/science/article/pii/0029554X69904467

[2] W. von der Linden, "Maximum-entropy data analysis," vol. 60, pp. 155–165.

[3] W. N. McElroy, S. Berg, T. Crockett, and R. G. Hawkins, "A COMPUTER-AUTOMATED ITERATIVE METHOD FOR NEUTRON FLUX SPECTRA DETERMINATION BY FOIL ACTIVATION. VOLUME 1. A STUDY OF THE ITERATIVE METHOD." [Online]. Available: https://apps.dtic.mil/sti/citations/AD0820556

[4] B. Pehlivanovic, S. Avdic, P. Marinkovic, S. A. Pozzi, and M. Flaska, "Comparison of unfolding approaches for monoenergetic and continuous fast-neutron energy spectra," vol. 49, pp. 109–114. [Online]. Available: https://www.sciencedirect.com/science/article/pii/S1350448712003575

[5] C. Cao, Q. Gan, J. Song, Q. Yang, L. Hu, F. Wang, and T. Zhou, "An adaptive deviation-resistant neutron spectrum unfolding method based on transfer learning," vol. 52, no. 11, pp. 2452–2459. [Online]. Available: https://www.sciencedirect.com/science/article/pii/S1738573319310137

[6] EJ-301, EJ-309 - Neutron/Gamma PSD Liquid Scintillators - Eljen Technology. [Online]. Available: https://eljentechnology.com/products/liquid-scintillators/ej-301-ej-309

[7] DT5730 / DT5730S - 8 Channel 14 bit 500 MS/s Digitizer. CAEN - Tools for Discovery. [Online]. Available: https://www.caen.it/products/dt5730/

[8] DT5533E - 4 Channel 4 kV/3 mA (4 W) Desktop HV Power Supply Module (USB/Ethernet). CAEN - Tools for Discovery. [Online]. Available: https://www.caen.it/products/dt5533e/

[9] GECO2020 - GEneral COntrol Software for CAEN HV Power Supplies. CAEN - Tools for Discovery. [Online]. Available: https://www.caen.it/products/geco2020/

[10] CoMPASS - Multiparametric DAQ Software for Physics Applications. CAEN - Tools for Discovery. [Online]. Available: https://www.caen.it/products/compass/

[11] J. H. Heltsley, L. Brandon, A. Galonsky, L. Heilbronn, B. A. Remington, S. Langer, A. Vander Molen, J. Yurkon, and J. Kasagi, "Particle identification via pulse-shape discrimination with a charge-integrating ADC," vol. 263, no. 2, pp. 441–445. [Online]. Available: https://www.sciencedirect.com/science/article/pii/0168900288909849

[12] G. Dietze and H. Klein, "Gamma-calibration of NE 213 scintillation counters," vol. 193, no. 3, pp. 549–556. [Online]. Available: https://www.sciencedirect.com/science/article/pii/0029554X8290249X

[13] S. A. Payne, W. W. Moses, S. Sheets, L. Ahle, N. J. Cherepy, B. Sturm, S. Dazeley, G. Bizarri, and W.-S. Choong, "Nonproportionality of Scintillator Detectors: Theory and Experiment. II," vol. 58, no. 6, pp. 3392–3402.

[14] F. Ben Bouallègue, J. F. Crouzet, and D. Mariano-Goulart, "A heuristic statistical stopping rule for iterative reconstruction in emission tomography," vol. 27, no. 1, pp. 84–95. [Online]. Available: https://doi.org/10.1007/s12149-012-0657-5

[15] L. Montgomery, A. Landry, G. Al Makdessi, F. Mathew, and J. Kildea, "A novel MLEM stopping criterion for unfolding neutron fluence spectra in radiation therapy," vol. 957, p. 163400. [Online]. Available: https://www.sciencedirect.com/science/article/pii/S0168900220300061

[16] R. Worrall, B. Colling, M. Gilbert, E. Litherland-Smith, C. Nobs, L. Packer, C. Wilson, and A. Zohar, "The development, testing and comparison of unfolding methods in SPECTRA-UF for neutron spectrometry," vol. 161, p. 112038. [Online]. Available: https://linkinghub.elsevier.com/retrieve/pii/S092037962030586X

VI. Code Availability

Both algorithms, an example script, and all data collected for this study have been provided on GitHub at the following link: https://github.com/tylerdolezal/Neutron-Unfolding.